Talanta 105 (2013) 34–39

Contents lists available at SciVerse ScienceDirect

Talanta

journal homepage: www.elsevier.com/locate/talanta

A novel dansyl-based fluorescent probe for highly selective detection of ferric ions

Min Yang [a,b], Mingtai Sun [b], Zhongping Zhang [a,b], Suhua Wang [a,b,*]

[a] Department of Chemistry, University of Science and Technology of China, Hefei, Anhui 230026, People's Republic of China
[b] Institute of Intelligent Machines, Chinese Academy of Sciences, Hefei, Anhui 230031, People's Republic of China

ARTICLE INFO

Article history:
Received 27 August 2012
Received in revised form
20 November 2012
Accepted 25 November 2012
Available online 1 December 2012

Keywords:
Dansyl-based fluorescent probe
Iron ion
Visual detection
Di-(2-picolyl)amine

ABSTRACT

A novel dansyl-based fluorescent probe was synthesized and characterized. It exhibits high selectivity and sensitivity towards Fe^{3+} ion. This fluorescent probe is photostable, water soluble and pH insensitive. The limit of detection is found to be 0.62 μM. These properties make it a good fluorescent probe for Fe^{3+} ion detection in both chemical and biological systems. Spike recovery test confirms its practical application in tap water samples.

1. Introduction

Many transition metals are important to the chemistry of living organisms, such as iron, molybdenum, zinc, etc. Iron is the most familiar transition metal that is found as the essential element in myoglobin, hemoglobin, cytochromes and plays roles in many biological processes, such as electron transfer reactions, gene regulation, oxygen transport, and regulation of cell growth and differentiation [1–3]. These functions are dependent on the iron homeostasis in human body, thus both iron deficiency and iron overload are harmful to human health [4–7]. The iron homeostasis is related to iron metabolism and iron uptake from dietary resources, therefore the determination of iron contents in food and drinks is important for human health.

The current methods for ion determination include atomic absorption spectroscopy [8], ion chromatography, colorimetry [9,10], spectrophotometry [11], and voltammetry [12]. These techniques need complicated procedures and expensive instruments. Fluorescent-based methods could be good alternatives for iron detection in many cases due to their high sensitivity, visualization capability, and ease of operation. Several fluorescent methods have been reported to detect Fe^{3+} ion, such as rhodamine-based probes [13–16], cumarin-based probes [17], graphene oxide-based probes [18,19], benzimididazole-based probes [20,21], fluorescent polymer-based probes [22], and gold nanoparticle-based probes [23]. Rhodamine-based fluorescent probes have bad water solubility and their usages in biological applications are limited. The fluorescence color of benzimididazole-based probes, fluorescent polymer-based probes, and gold nanoparticle-based probes is blue, which is not suitable for biological imaging. These organic fluorescent probes are also synthesized through several steps and the structures of the probes are complicated. So it is still a challenge however to design simple, hydrophilic, selective, and sensitive fluorescent probes for Fe^{3+} ion.

Dansyl fluorophore is widely used in amino acids modification, protein sequencing and amino analysis, because of its high fluorescence quantum yields and large Stokes shift. A couple of dansyl-based probes for the detection of Zn^{2+} have been reported [24,25]. Herein, we report a novel dansyl-based fluorescent probe which shows high selectivity and sensitivity for the detection of Fe^{3+} ion. In the probe, the dansyl moiety functions as a fluorescent reporter and an electron-rich moiety as a receptor to response to Fe^{3+} ion. The dansyl-based fluorescent probe exhibits a high selectivity for Fe^{3+} ion over other metal ions. The limit of detection is measured to be 0.62 μM based on the definition of three times the deviation of the blank signal, which is more sensitive than other organic probes for Fe^{3+} ion detection [19,20,23].

2. Experimental

2.1. Materials and chemicals

All chemicals were of analytical grade and used without further purification. Di-(2-picolyl)amine was purchased from Sigma. Dansyl chloride was purchased from Shanghai Sangon Biotechnology Co. Ltd. The solutions of metal ions were prepared

* Corresponding author at: Chinese Academy of Sciences, Institute of Intelligent Machines, Science island, Hefei City, Anhui, Hefei, China. Tel.: +86 551 5591 812; fax: +86 551 5591 156.
E-mail address: shwang@iim.ac.cn (S. Wang).

0039-9140/$ - see front matter © 2012 Elsevier B.V. All rights reserved.
http://dx.doi.org/10.1016/j.talanta.2012.11.066

from KCl, $CaCl_2$, NaCl, $CoCl_2 \cdot 6H_2O$, $FeCl_3 \cdot 6H_2O$, $ZnCl_2$, $LiCl \cdot H_2O$, $MgCl_2 \cdot 6H_2O$, $BaCl_2 \cdot 2H_2O$, $NiCl_2 \cdot 6H_2O$, and $FeSO_4 \cdot 7H_2O$ respectively. All the solutions were prepared with ultrapure water purified by a Millipore water purification system (18.2 MΩ cm).

2.2. Apparatus

^{1}H NMR spectra were recorded on a Brucker Avance 400 MHz. Mass spectrum was obtained on a Thermo Proteome X-LTQ MS. Fluorescence experiments were carried out on a Perkin Elmer LS-55 luminescence spectrometer. The UV–vis absorption spectra were obtained with a Shimadzu UV-2550 spectrometer. IR data were collected on Thermo Scientific iS10 infrared spectrometer. The pH values were measured by PHS-3C. Photographs were taken by a Canon 350D digital camera.

2.3. Synthesis of the dansyl-based fluorescent probe

The dansyl-based fluorescent probe, 5-(dimethylamino)-*N*,*N*-bis(pyridin-2-ylmethyl) naphthalene-1-sulfonamide (Ds-DPA), was synthesized by mixing 134.9 mg (0.5 mmol) of dansyl chloride and 90 μL (0.5 mmol) of di-(2-picolyl)amine in 5 mL of dichloromethane containing 69.7 μL (0.5 mmol) of triethylamine (TEA) in a 25 mL round bottom flask. The mixture was stirred under N_2 for 2 h at room temperature. The solvent was then evaporated to dry on a rotary evaporator. The product was purified using column chromatography on silica, eluting with dichloromethane/methanol (40:1 v/v). Completed evaporation of the solvent produced the dansyl-based probe as green oil (128 mg, 54.5%). R_f=0.42 (40:1 dichloromethane/methanol). ^{1}H NMR (400 MHz, $CDCl_3$, ppm): δ 2.87 (s, 6H), 4.73 (s, 4H), 7.00–7.04 (q, 2H, J=5.0 Hz), 7.15–7.17 (m, 3H, J=6.8 Hz), 7.40–7.45 (q, 3H, J=7.4 Hz), 7.50–7.54 (t, H, J=7.8 Hz), 8.21–8.23 (d, H, J=7.2 Hz), 8.34–8.35 (d, 2H, J=5.6 Hz), 8.38–8.40 (d, H, J=8.8 Hz), 8.47–8.50 (d, H, J=8.6 Hz). MS (m/z): calculated 432.16, found 433.16 ($M+H^+$).

2.4. Fluorescence experiments

A stock solution of Ds-DPA (30 mM) in ethanol was prepared. Stock solutions of various metal ions were prepared by dissolving their salts in ultrapure water. The working solution of Ds-DPA (0.9 μM) was prepared by diluting 6 μL of the Ds-DPA stock solution in 2 mL 50% (v/v) water–ethanol mixture. The metal ion solutions were added into the probe solutions followed by recording the fluorescence spectra. All fluorescence spectra were recorded in the range from 400 nm to 700 nm using a 340 nm excitation wavelength and a 500 nm/min scan rate.

3. Results and discussion

3.1. Characterization of fluorescent Ds-DPA

The highly fluorescent Ds-DPA was synthesized by the reaction between the nonfluorescent dansyl chloride and di-(2-picolyl)-amine under mild conditions (Scheme 1). Fig. 1 shows the excitation and emission spectra of Ds-DPA in 50% (v/v) water–ethanol solution. Clearly, the maximum excitation and emission are at 340 nm and 550 nm, respectively, showing a very large Stokes shift. The emission spectrum of Ds-DPA probe is nearly symmetric and the width of the half height is 108 nm. The fluorescence quantum yield (QY) of Ds-DPA was measured to be (38.1 ± 3.1) % using fluorescein as standard (QY is 95% in 0.1 M NaOH) (Fig. S1) [26,27]. The fluorescent probe shows a relatively high quantum yield and is suited for biological detection and imaging. Fig. 2 shows the UV–vis spectra of Ds-DPA, dansyl chloride and di-(2-picolyl)amine. Ds-DPA has three absorption peaks at 214 nm, 255 nm, 340 nm, which are different from both the dansyl chloride and di-(2-picolyl)amine. Dansyl chloride has three absorption peaks at 208 nm, 258 nm, and 362.5 nm. Di-(2-picolyl)amine has a absorption maximum at 265.5 nm. The structure of Ds-DPA was also confirmed using IR spectrometry (Fig. S2). The vibration bands at 1322 cm^{-1} and 1143 cm^{-1} can be assigned to symmetric and asymmetric stretching of sulfonamides groups [28]. The ESI-MS spectrum reveals the dominant species at m/z=433.16 ($M+H^+$), which is in consistent with the Ds-DPA molecular formula (Fig. S3). The ^{1}H NMR spectrum suggests the purity of the product and confirms the chemical structure of Ds-DPA (Fig. S4).

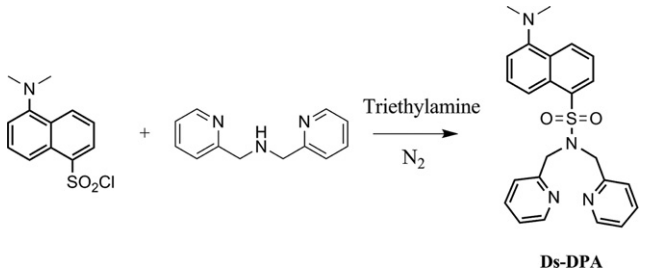

Scheme 1. The synthesis of fluorescent Ds-DPA under N_2 for 2 h at room temperature.

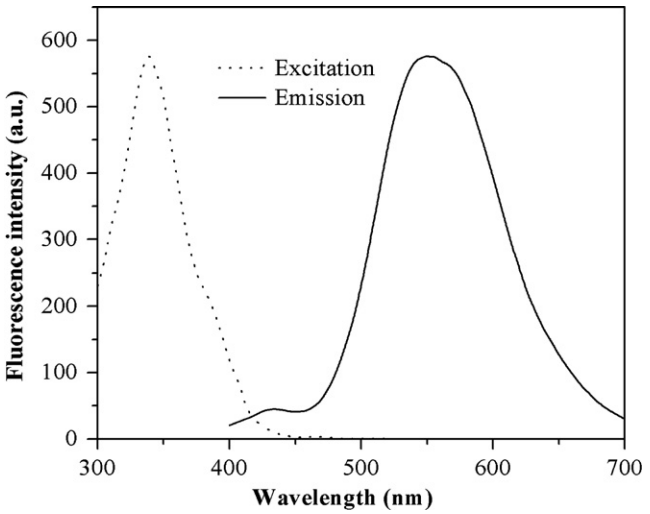

Fig. 1. Excitation spectra and emission spectra of Ds-DPA (1.5 μM) in 2 mL 50% (v/v) water–ethanol solution. The dot line is the excitation spectra, and the solid line is the emission spectra. The maximum excitation and emission are at 340 nm and 550 nm, respectively.

3.2. Fluorescence stability of Ds-DPA

Many organic fluorescent probes are sensitive to pH, so the influence of pH on the fluorescence intensity of Ds-DPA has been investigated in phosphate buffer–ethanol (50%, v/v) solution (Fig. S5). The fluorescence intensities are nearly same in the pH range from 3 to 11, suggesting that the fluorescence of Ds-DPA is pH insensitive and this fluorescent probe has potential applications in biological imaging. The photostability of Ds-DPA was also investigated by irradiating its solution (0.9 μM) under a Xenon light source with a power of 20 kW. The fluorescence intensity of Ds-DPA was recorded each minute for two hours during the

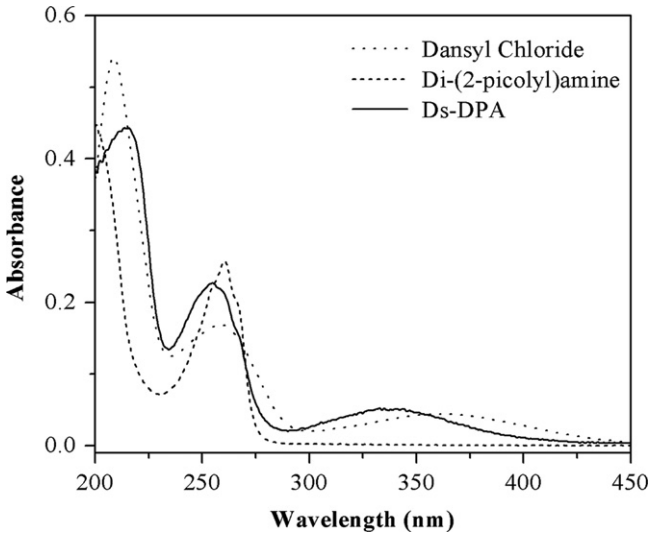

Fig. 2. The absorption spectra of Ds-DPA, dansyl chloride and di-(2-picolyl) amine in 3 mL 50% (v/v) water–ethanol solution. The maximum absorption of Ds-DPA is at 214 nm, 255 nm and 340 nm.

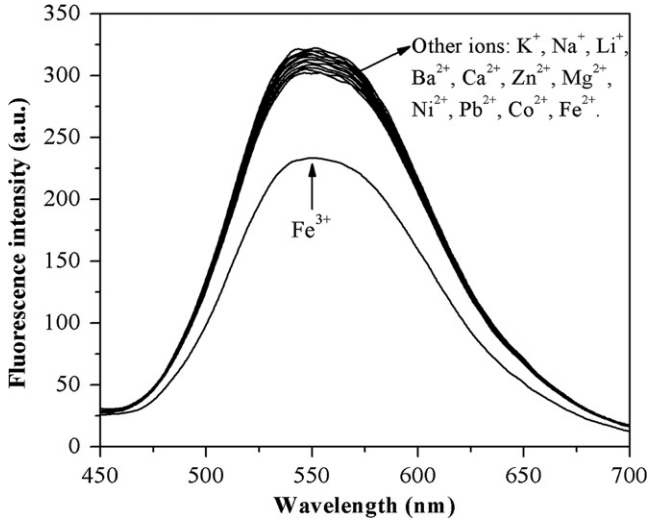

Fig. 3. Fluorescence responses of Ds-DPA (0.9 μM) in the presence of different metal ions (25 μM) in 2 mL 50% (v/v) water–ethanol solution.

ultraviolet light irradiation (Fig. S6). The result clearly shows that the fluorescence intensity is almost retained after 100 times of consecutive illumination (1 min for each time), indicating the Ds-DPA fluorescence probe has a good photostability and is resistant to photobleaching.

3.3. Selective fluorescence quenching by ferric ions

To investigate the selectivity of Ds-DPA towards different metal ions, other metal ions were added into the solution of the fluorescent probe under the same conditions. It can be seen from Fig. 3 that the addition of other metal ions (K^+, Na^+, Li^+, Ba^{2+}, Ca^{2+}, Zn^{2+}, Mg^{2+}, Ni^{2+}, Pb^{2+}, Co^{2+}, Fe^{2+}) do not induce obvious fluorescence decrease. However, the adding of the same concentration of Fe^{3+} ion (25 μM) caused the quench effect on the fluorescence intensity of Ds-DPA, implying that Fe^{3+} ion can effectively quench the fluorescence of Ds-DPA. This result indicates that Ds-DPA shows high selectivity towards Fe^{3+} ion and has the potential to be used to detect Fe^{3+} ion in many aspects.

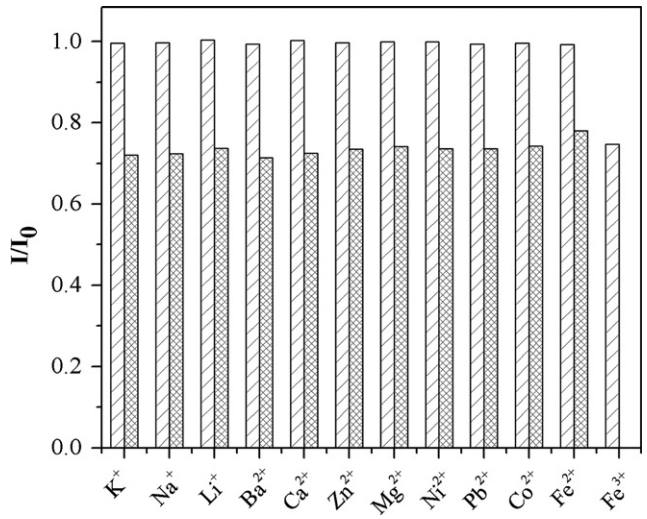

Fig. 4. Fluorescence responses of Ds-DPA (0.9 μM) to Fe^{3+} (30 μM) in the presence of other metal ions (the dense bar portion). The sparse bar presents the fluorescence response of Ds-DPA to other metal ions (150 μM). I: fluorescence intensity of Ds-DPA after adding metal ions, I_0: fluorescence intensity of Ds-DPA before adding metal ions.

3.4. Interference study

There are sometimes several kinds of metal ions coexisting in the same system, those metal ions may interfere the detection of the target ions. To further validate the selectivity and anti-interference of Ds-DPA towards Fe^{3+} ion, competition experiments were carried out by adding Fe^{3+} (30 μM) to the solution of Ds-DPA in the presence of other metal ions (150 μM). Result in Fig. 4 revealed that the quenching effect of Fe^{3+} ion was not affected in the presence of other metal ions. Moreover, Ds-DPA can discriminate Fe^{2+} ion with Fe^{3+} ion. Thereby, Ds-DPA has a high selectivity towards Fe^{3+} ion. This property makes Ds-DPA an ideal fluorescent probe for Fe^{3+} ion detection in chemical and biological systems.

3.5. Dose response of the fluorescence of Ds-DPA to Fe^{3+}

The fluorescence of Ds-DPA was quenched by Fe^{3+} ion in a dose-response relationship. Fig. 5 displays the changes of fluorescence spectra of Ds-DPA upon the addition of Fe^{3+} ions in 50% (v/v) water–ethanol solution. The inset is the calibration curve corresponding to the fluorescence intensity versus the concentration of Fe^{3+} ion. A linear relationship (R=0.9995) can be obtained in concentration range below 25 μM, as shown in Fig. 6. The limit of detection (LOD) was found to be 0.62 μM based on the definition of three times the deviation of the blank signal, which was lower than that of the Ion Chromatography method (1.2 μM) [29]. This result shows that the method has high sensitivity for Fe^{3+} ion detection. Furthermore, the fluorescence color changes of Ds-DPA solution upon different amounts of Fe^{3+} ion have also been studied in order to establish a visual detection method. Fig. 7 shows the dependence of the fluorescence color of Ds-DPA solution on the addition of different amounts of Fe^{3+} ion. Clearly, the color gradually fades as the concentration of Fe^{3+} ion increases, and finally disappears when the concentration of Fe^{3+} increases to 1.0 mM. So the result indicates that the fluorescent probe can be capable for visual detection of Fe^{3+} ions.

3.6. The quenching mechanism of Fe^{3+} ion

There are two major pathways to quench the fluorescence of the fluorescent probe, one is energy transfer pathway and the

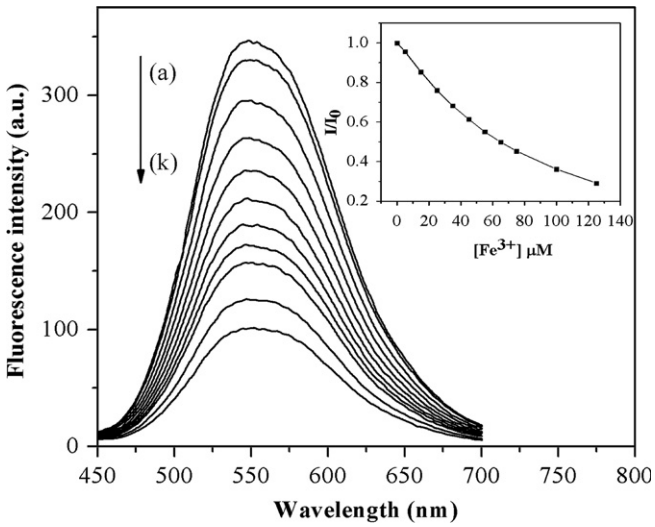

Fig. 5. Fluorescence responses of Ds-DPA (0.9 μM) upon adding different concentrations of Fe^{3+} ion, (a) Ds-DPA only, (b)–(k) 5 μM, 15 μM, 25 μM, 35 μM, 45 μM, 55 μM, 65 μM, 75 μM, 100μM, 125μM Fe^{3+} ion. I: fluorescence intensity of Ds-DPA after adding Fe^{3+} ion, I_0: fluorescence intensity of Ds-DPA before adding Fe^{3+} ion. The inset plot is the calibration curve corresponding to the fluorescence intensity of the Ds-DPA versus the concentration of Fe^{3+} ion.

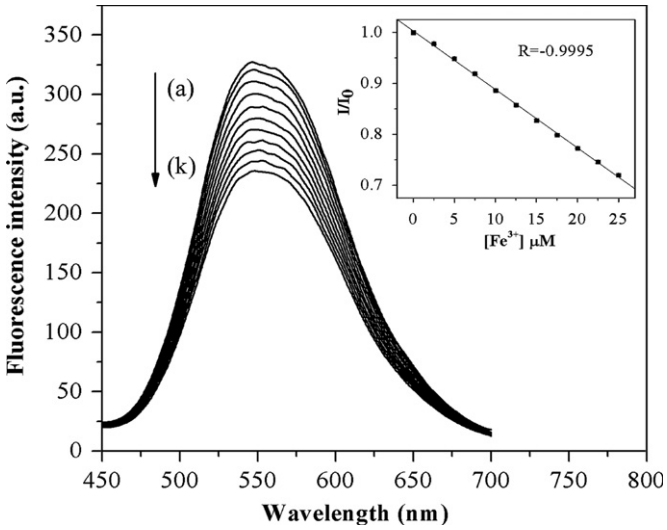

Fig. 6. Fluorescence responses of Ds-DPA (0.9 μM) upon adding different concentrations of Fe^{3+} ion, (a) Ds-DPA only, (b)–(k) 2. 5 μM, 5 μM, 7.5 μM, 10 μM, 12.5 μM, 15 μM, 17.5 μM, 20 μM, 22.5μM, 25μM Fe^{3+} ion. I: fluorescence intensity of Ds-DPA after adding Fe^{3+} ion, I_0: fluorescence intensity of Ds-DPA before adding Fe^{3+} ion. The inset plot is the calibration curve corresponding to the fluorescence intensity of the Ds-DPA versus the concentration of Fe^{3+} ion.

other is electron transfer pathway. There is minimal spectra overlap between the emission spectra of Ds-DPA and the absorption spectra of Fe^{3+} ion, so fluorescence resonance energy transfer (FRET) is not the dominant pathway of quenching. Di-(2-picolyl)amine is a very strong nucleophile and can act as an electron donor. Fe^{3+} ion has strong electron-accepting ability and can capture electron easily. It is believed that the mechanism of quenching effect of Fe^{3+} ion may be attributed to electron transfer (ET) between Fe^{3+} ion and the excited Ds-DPA. To examine the quenching mechanism, we have synthesized a similar fluorescent probe, 5-(dimethylamino)-*N*,*N*-diethylnaphthalene-1-sulfonamide (Ds-DEA), by replacing the DPA moiety with diethylamine which is a weaker electron donor. So the probability of electron transfer between ferric ions and the Ds-DEA molecules is much less than the Ds-DPA. Fig. 8 shows the responses of the Ds-DEA fluorescent probe to different concentrations of ferric ions and the

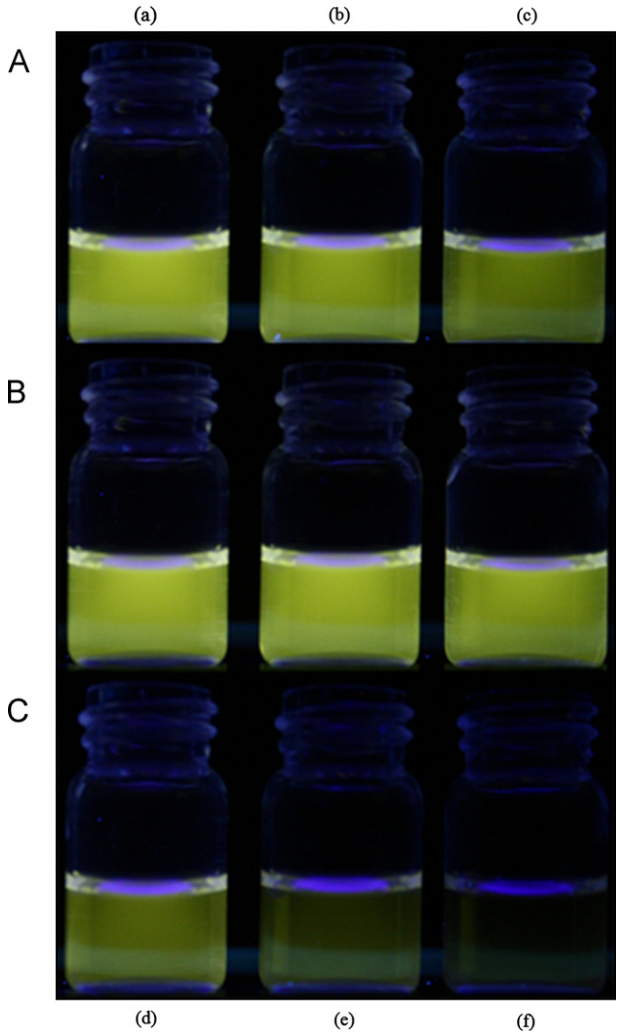

Fig. 7. Visual detection of Fe^{3+} ion under the 365 nm UV lamp illumination. (B): 0.9 μM of Ds-DPA in 1 mL 50% (v/v) water–ethanol solution as the blank control. (A), (C) the color change of Ds-DPA upon adding different concentrations of Fe^{3+} ion, (a)–(f) 0.03 mM, 0.06 mM, 0.1 mM, 0.23 mM, 0.46 mM, 1.0 mM Fe^{3+} ion.

comparison between Ds-DPA. It can be seen that the fluorescence of Ds-DPA quickly decreases in a fast manner compared with that of the Ds-DEA probe upon the addition of ferric ion. This result indicates that the electron transfer between Ds-DPA and ferric ion partially contributes to the fluorescence quenching. The fluorescence of Ds-DEA also gradually decreases upon the addition of ferric ion, implying that the absorbance of ferric ions at the excitation wavelength contributes to the decrease of the fluorescence.

In fact, the effect of absorbance of ferric ions on the fluorescence of dansyl chloride has been studied by Lohani and Lee [30]. They have found that the decrease in fluorescence intensity of the fluorophores without a receptor is mainly due to the absorbance of ferric ions. The contribution of the absorbance of excitation light by ferric ions to the decrease of fluorescence can be confirmed with the following experiments. Ferric ions can be chelated with Ethylene Diamine Tetraacetic Acid (EDTA), an effective chelating ligand for ferric ion, to form a stable complex and the ferric ion in the complex losses the ability to accept electrons. The addition of EDTA into the mixture solution of Ds-DEA and Fe^{3+} ions with weak fluorescence could not increase the fluorescence intensity (Fig. 9). This result clearly shows that the decrease of the fluorescence of Ds-DEA is not caused by electron transfer. When EDTA was added into the mixture solution of Ds-DPA and ferric ions with weak fluorescence, however,

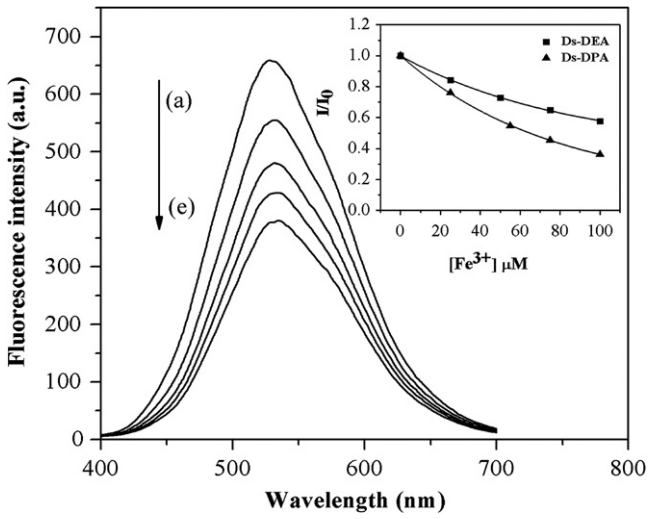

Fig. 8. Fluorescence responses of Ds-DEA upon adding different concentrations of Fe^{3+}, (a) Ds-DEA only, (b)–(e) 25 μM, 50 μM, 75 μM, 100 μM Fe^{3+} ion. I: fluorescence intensity of Ds-DEA after adding Fe^{3+} ion, I_0: fluorescence intensity of Ds-DEA before adding Fe^{3+} ion. Inset is the comparison between Ds-DEA and Ds-DPA under the same concentration of Fe^{3+}.

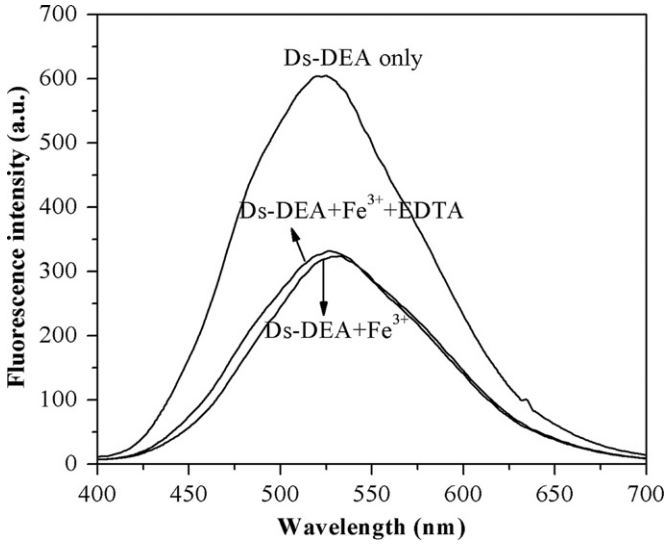

Fig. 9. Fluorescence spectra of Ds-DEA in the presence of Fe^{3+} ion (125 μM) and/or EDTA (250 μM) in 50% water–ethanol (v/v) solution.

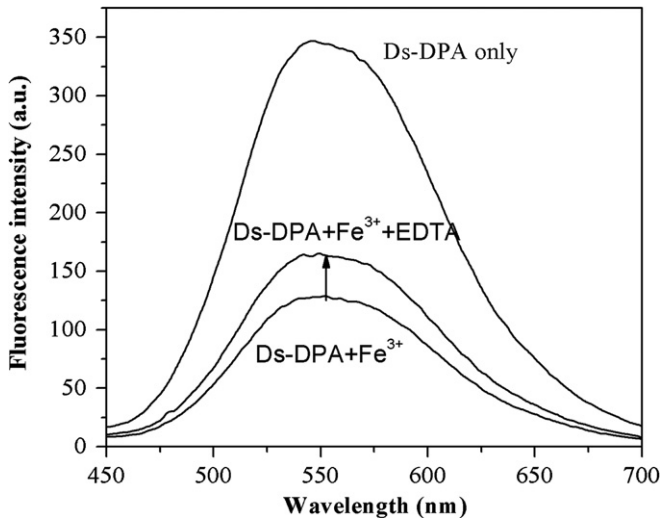

Fig. 10. Fluorescence spectra of Ds-DPA in the presence of Fe^{3+} ion (125 μM) and/or EDTA (250 μM) in 50% water–ethanol (v/v) solution.

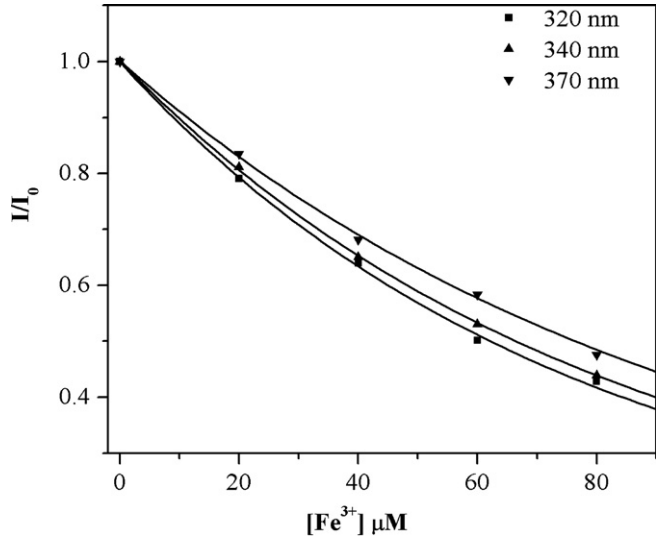

Fig. 11. The quench effects of ferric ions at various concentrations under different excitation wavelengths (320 nm, 340 nm, 370 nm).

the fluorescence of Ds-DPA increased by ~20%, as shown in Fig. 10. These results clearly suggest that the electron transfer occurs between Ds-DPA and ferric ion, which is consistent with the fact that the probability of electron transfer between ferric ion and Ds-DPA is much higher than Ds-DEA.

Although the decreased fluorescence of the Ds-DPA by ferric ions can be partially recovered by the addition of EDTA, the fluorescence cannot be recovered to its initial full intensity. This result implies that the absorbance of ferric ion at the excitation wavelength also contributes to the decrease of the fluorescence. This can be further confirmed by further experiments with different excitation wavelength, at which the ferric ion has different absorption coefficient. Fig. 11 shows that the fluorescence quenching efficiency of ferric ion with identical concentration decreases when the excitation wavelength changes from 320 nm to 340 nm and 370 nm. The quenching effect at 320 nm is greater than those at 340 nm and 370 nm, consistent with that the absorbance of ferric ion is higher at 320 nm than those at 340 and 370 nm (Fig. S7). All the results reveal that the absorbance of ferric ion at the excitation wavelength also causes the decrease of the fluorescence. Therefore, the decrease of fluorescence of Ds-DPA by the addition of ferric ion could be attributed to the absorbance of ferric ion at the excitation wavelength and the electron transfer between DPA and ferric ion.

3.7. Spike and recovery test of Fe^{3+} ion in tap water

The Ds-DPA fluorescent probe has been validated for practical applications in the determination of Fe^{3+} ion content in local tap water samples. Control experiments show that tap water itself has no quenching effect on the fluorescence of the probe, so the tap water has been directly used without pretreatment for the spike and recovery test (Fig. S9). Ferric ion was added into the tap water samples containing Ds-DPA and the final concentrations of ferric ions were 5 μM, 10 μM, 15 μM, and 20 μM. The fluorescence intensities of Ds-DPA were recorded before and after the addition of Fe^{3+} ion. The fluorescence spectra of Ds-DPA to different spiked tap water samples were showed in Fig. 12 and the contents of Fe^{3+} ion were recovered using the linear equation

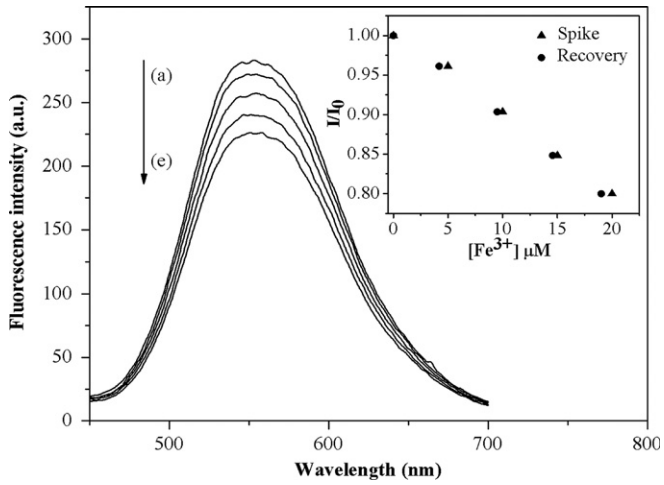

Fig. 12. Fluorescence intensity of Ds-DPA responses to different tap water samples, (a) Ds-DPA only, (b)–(e) sample 1, sample 2, sample 3, and sample 4. Inset is the comparison between the spike concentration and the recovery concentration of ferric ion.

Table 1
Spike and recovery test in tap water.

Tap water sample	Fe^{3+} added (μM)	Fe^{3+} found (μM)	RSD (%, $n=3$)	Recovery (%)
Sample 1	5.00	4.19	6.48	83.8
Sample 2	10.00	9.49	5.39	94.9
Sample 3	15.00	14.57	2.36	97.2
Sample 4	20.00	19.01	4.23	95.1

Table 2
Spike and recovery test in diluted tap water.

Tap water sample	Fe^{3+} added (μM)	Fe^{3+} found (μM)	RSD (%, $n=5$)	Recovery (%)
Sample 1	5.00	4.87	5.29	97.5
Sample 2	10.00	10.26	5.98	102.6
Sample 3	15.00	15.34	3.91	102.3
Sample 4	20.00	20.32	3.02	101.6

obtained in Fig. 6. Table 1 presents the results and it can be seen that it has a good recovery at the concentrations of 10 μM, 15 μM, and 20 μM. We have found that the local tap water displays weak fluorescence maxima at 430nm which could be due to some bacteria and organic contaminants, as shown in the Fig. S10. The background fluorescence can be greatly reduced by diluting 10 times and is comparable with that of ultrapure water. For comparison, the spike and recovery test has also been carried using diluted tap water which was shown in Table 2. The results are nearly the same as those with un-pretreated tap water. This result demonstrates that Ds-DPA has the potential to be used to selectively and sensitively determine Fe^{3+} ion in real water samples.

4. Conclusions

In summary, the dansyl-based fluorescent probe for Fe^{3+} ion was synthesized and evaluated successfully. The fluorescent probe exhibits high sensitivity and selectivity to ferric ions over other transition metals. The limit of detection of Ds-DPA is 0.62 μM and is much lower than the recommended standard value for Fe^{3+} in drinking water (5.4 μM or 0.3 mg/L) [10]. It has the potential to be used to detect Fe^{3+} ion in tap water. Due to its high photostability, pH insensitivity, and water soluble properties, fluorescent Ds-DPA can be applied to biological and chemical systems.

Acknowledgments

This work was supported by the National Basic Research Program of China (2011CB933700), the Natural Science Foundation of China (No.s 21077108, 21173229) and the Innovation Project of the Chinese Academy of Sciences (KJCX2-YW-H29).

Appendix A. Supporting information

Supplementary data associated with this article can be found in the online version at http://dx.doi.org/10.1016/j.talanta.2012.11.066.

References

[1] J.L. Beard, J. Nutr. 131 (2001) 568S–579S.
[2] A.S. Zhang, C.A. Enns, J. Biol. Chem. 284 (2008) 711–715.
[3] J.D. Haas, T. Browlie IV, J. Nutr. 131 (2001) 676S–690S.
[4] R. Evstatiev, C. Gasche, Gut 61 (2012) 933–952.
[5] J.R. Burdo, J.R. Connor, BioMetals 16 (2003) 63–75.
[6] T. Moos, E.H. Morgan, Ann. N.Y. Acad. Sci. 1012 (2004) 14–26.
[7] G. Papanikolaou, K. Papanikolaou, Toxicol. Appl. Pharmacol. 202 (2005) 199–211.
[8] O. Akira, I. Hiromi, K. Chikako, I. Hisanori, O. Kousaburo, Talanta 65 (2005) 525–530.
[9] Z.Q. Liang, C.X. Wang, J.X. Yang, H.W. Gao, Y.P Tian, X.T. Tao, M.H. Jiang, New J. Chem. 31 (2007) 906–910.
[10] D.B. Wei, Y.L. Sun, J.X. Yin, G.H. Wei, Y.G. Du, Sens. Actuators B 160 (2011) 1316–1321.
[11] S. Lunvongsa, M. Oshima, S. Motomizu, Talanta 68 (2006) 969–973.
[12] A. Bobrowski, K. Nowak, J. Zarebski, Anal. Bioanal. Chem. 382 (2005) 1691–1697.
[13] Z. Aydin, Y.B. Wei, M.L. Guo, Inorg. Chem. Commun. 20 (2012) 93–96.
[14] L.Z. Zhang, J.Y. Wwang, J.L. Fan, K.X. Guo, X.J. Peng, Bioorg. Med. Chem. Lett. 21 (2011) 5413–5416.
[15] Z.Q. Hu, Y.C. Feng, H.Q. Huang, L. Ding, X.M. Wang, C.S. Lin, M. Li, C.P. Ma, Sens. Actuators B 156 (2011) 428–432.
[16] A.J. Weerasinghe, C. Schmiesing, S. Varaganti, G. Ramakrishna, E. Sinn, J. Phys. Chem. B 114 (2010) 9413–9419.
[17] J.N. Yao, W. Dou, W.W. Qin, W.S. Liu, Inorg. Chem. Commun. 12 (2009) 116–118.
[18] Q.S. Mei, C.L. Jiang, G.J. Guan, K. Zhang, B.H. Liu, R.Y. Liu, Z.P. Zhang, Chem. Commun. 48 (2012) 7468–7470.
[19] D. Wang, L. Wang, X.Y. Dong, Z. Shi, J. Jin, Carbon 50 (2012) 2147–2154.
[20] W.Y. Lin, L.L. Long, L. Yuan, Z.M. Cao, J.B. Feng, Anal. Chim. Acta 634 (2009) 262–266.
[21] D.Y. Lee, N. Singh, D.O. Jang, Tetrahedron Lett. 52 (2011) 1368–1371.
[22] A.K. Dwivedi, G. Saikia, P.K. Iyer, J. Mater. Chem. 21 (2011) 2502–2507.
[23] S.P. Wu, Y.P. Chen, Y.M. Sung, Analyst 136 (2011) 1887–1891.
[24] T. Koike, T. Watanabe, S. Aoki, E. Kimura, M. Shiro, J. Am. Chem. Soc. 118 (1996) 12696–12703.
[25] P.J. Jiang, L.Z. Chen, J. Lin, Q. Liu, J. Ding, X. Gao, Z.J. Guo, Chem. Commun. (2002) 1424–1425.
[26] S.H. Wang, M.Y. Han, D.J. Huang, J. Am. Chem. Soc. 131 (2009) 11692–11694.
[27] A.M. Brouwer, Pure Appl. Chem. 83 (2011) 2213–2228.
[28] K. Nakanishi et al., Infrared Absorption Spectroscopy, 2nd Holden-Day, 1977.
[29] C.O. Moses, A.T. Herlihy, J.S. Herman, A.L. Mills, Talanta 35 (1988) 15–22.
[30] C.R. Lohani, K.H. Lee, Sens. Actuators B 143 (2010) 649–654.